Bioorganic & Medicinal Chemistry Letters 30 (2020) 127502

Contents lists available at ScienceDirect

Bioorganic & Medicinal Chemistry Letters

journal homepage: www.elsevier.com/locate/bmcl

Antimalarial activity of tetrahydro-β-carbolines targeting the ATP binding pocket of the *Plasmodium falciparum* heat shock 90 protein

Scott Eagon[a,*], Jared T. Hammill[b], Jordan Bach[a], Nikalet Everson[c], Tyler A. Sisley[d,e], Michael J. Walls[f], Sierra Durham[g], Dylan R. Pillai[h], Mofolusho O. Falade[b], Amy L. Rice[b], Joshua J. Kimball[c], Horacio Lazaro[c], Celine DiBernardo[a], R. Kiplin Guy[b]

[a] Department of Chemistry and Biochemistry, California Polytechnic State University, San Luis Obispo, CA 93407, USA
[b] Department of Pharmaceutical Sciences, University of Kentucky, Lexington, KY 40508, USA
[c] Promega Biosciences, 277 Granada Drive, San Luis Obispo, CA 93401, USA
[d] Department of Chemistry and Chemical Biology, Harvard University, Cambridge, MA 02138, USA
[e] Department of Microbiology, Harvard Medical School, Boston, MA 02115, USA
[f] Department of Public Health, Tauro University, Vallejo, CA 94592, USA
[g] Department of Food Science and Technology, University of California Davis, Davis, CA 95616, USA
[h] Department of Pathology and Laboratory Medicine, University of Calgary, Calgary, Alberta, Canada

ARTICLE INFO

Keywords:
Malaria
Plasmodium falciparum
Tetrahydro-β-carbolines
Structure activity relationship
Structure based design

ABSTRACT

A series of tetrahydro-β-carboline derivatives of a lead compound known to target the heat shock 90 protein of Plasmodium falciparum were synthesized and assayed for both potency against the parasite and toxicity against a human cell line. Using a rationalized structure based design strategy, a new lead compound with a potency two orders of magnitude greater than the original lead compound was found. Additional modeling of this new lead compound suggests multiple avenues to further increase potency against this target, potentially paving the path for a therapeutic with a mode of action different than any current clinical treatment.

Malaria is caused by protozoan parasites of the *Plasmodium* genus, with *P. falciparum* and *P. vivax* responsible for vast majority of cases. In 2018, an estimated 228 million cases and 405,000 deaths were caused by *Plasmodium*, with most deaths occurring in young children and pregnant women.[1] *P. falciparum* is by far the most deadly, accounting for approximately 90% of all deaths worldwide.[2] Despite a world-wide effort to combat this deadly disease, a number of clinical challenges have prevented further progress in the battle to eliminate the disease. In particular, the absence of a clinically useful vaccine,[3] the complexity of the *Plasmodium* lifecycle,[4] emergence of strains resistant to artemisinin-based combination therapies (ACTs)[5] and a small number of validated small molecule targets[6] underscore the need for treatments with new modes of action.

Heat shock proteins (Hsp) are a major class of chaperone proteins found in all life forms ranging from prokaryotes to humans with heat shock protein 90 (Hsp90) being one of the most common of all such proteins.[7] Since the malaria parasite must be transmitted from a poikilothermic mosquito to a homothermic human, heat shock proteins are vital for the parasite to survive the change in temperature. In fact, a few degrees of temperature change can cause the *P. falciparum* heat shock 90 protein (PfHsp90) transcription rate to more than triple.[8] The ATP binding pocket of PfHsp90 is highly conserved among a number of clinical isolates, underscoring the critical cellular function of this chaperone protein.[9] A few small molecule inhibitors of PfHsp90, most notably geldanamycin, are known to be potent anti-malarial agents. However, unacceptable toxicity profiles preclude the use of these compounds in the clinic.[10] Still, the critical role of PfHsp90 in parasite viability and the fact that no current clinical treatment possesses a similar mechanism of action both make this an attractive small-molecule target.

Our group previously reported that the β-carboline harmine binds selectively to the PfHsp90 ATP binding domain relative to human Hsp90.[11] We developed a microwave-mediated methodology to readily prepare a library of tetrahydro-β-carboline and β-carboline derivatives of the Harmine scaffold[12] and tested a number of compounds to assay their antimalarial activity. Our most potent compound from this initial collection was **1**, a 5-chloro-tetrahydro-β-carboline derivative of harmine that displayed modest activity and low toxicity against human cells (Fig. 1).[13]

To design a more potent second generation of inhibitors, we first

* Corresponding author.
E-mail address: seagon@calpoly.edu (S. Eagon).

https://doi.org/10.1016/j.bmcl.2020.127502
Received 14 July 2020; Received in revised form 12 August 2020; Accepted 16 August 2020
Available online 18 August 2020
0960-894X/

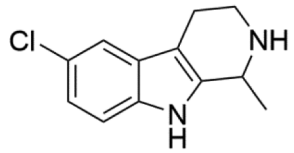

(1)

3D7 EC_{50} = 12.2 ± 2.3μM

HepG2 EC_{50} = 160 ± 10μM

HeLa EC_{50} = 1100 ± 300μM

Fig. 1. Structure, cytotoxicity and antimalarial activity of initial lead compound **1**.

attempted to rationalize a pharmacophore model of **1**. Fortunately, a solved protein structure for the *N*-terminus region of PfHsp90 bound to ADP is available (PDB ID: 3 k60, Fig. 2). The adenine heterocycle is the most deeply embedded end of the ADP molecule, making polar contacts with residues Thr171 and Asp79. Below the adenine rings, isoleucine and phenylalanine residues form an aliphatic floor, although ADP itself does not appear to interact with these hydrophobic residues. The more polar phosphate end of ADP makes several polar contacts with Arg98 and Asn37, and extends away from the depths of the pocket, presumably exposed to solvent. Given that both adenine and harmine share a similar fused 5- and 6-membered heterocyclic system, we hypothesized that **1** was binding in similar fashion, presumably making polar contact with the same Asp79 and Thr171 residues (Fig. 2). While this binding model is highly speculative, it suggests two potential paths to increase potency. One path would be substituting larger aromatic/aliphatic groups at the methyl position of **1** to take advantage of the aliphatic floor formed by Ile77 and Phe124. A second approach could be the introduction of new groups at the 5-chloro position to take advantage of the polar residues that interact with the phosphate group of the native ligand. Since it is synthetically easier to vary the methyl position of **1**, we decided to concentrate on synthesizing a library of compounds with various phenyl rings in place of the methyl group of **1**.

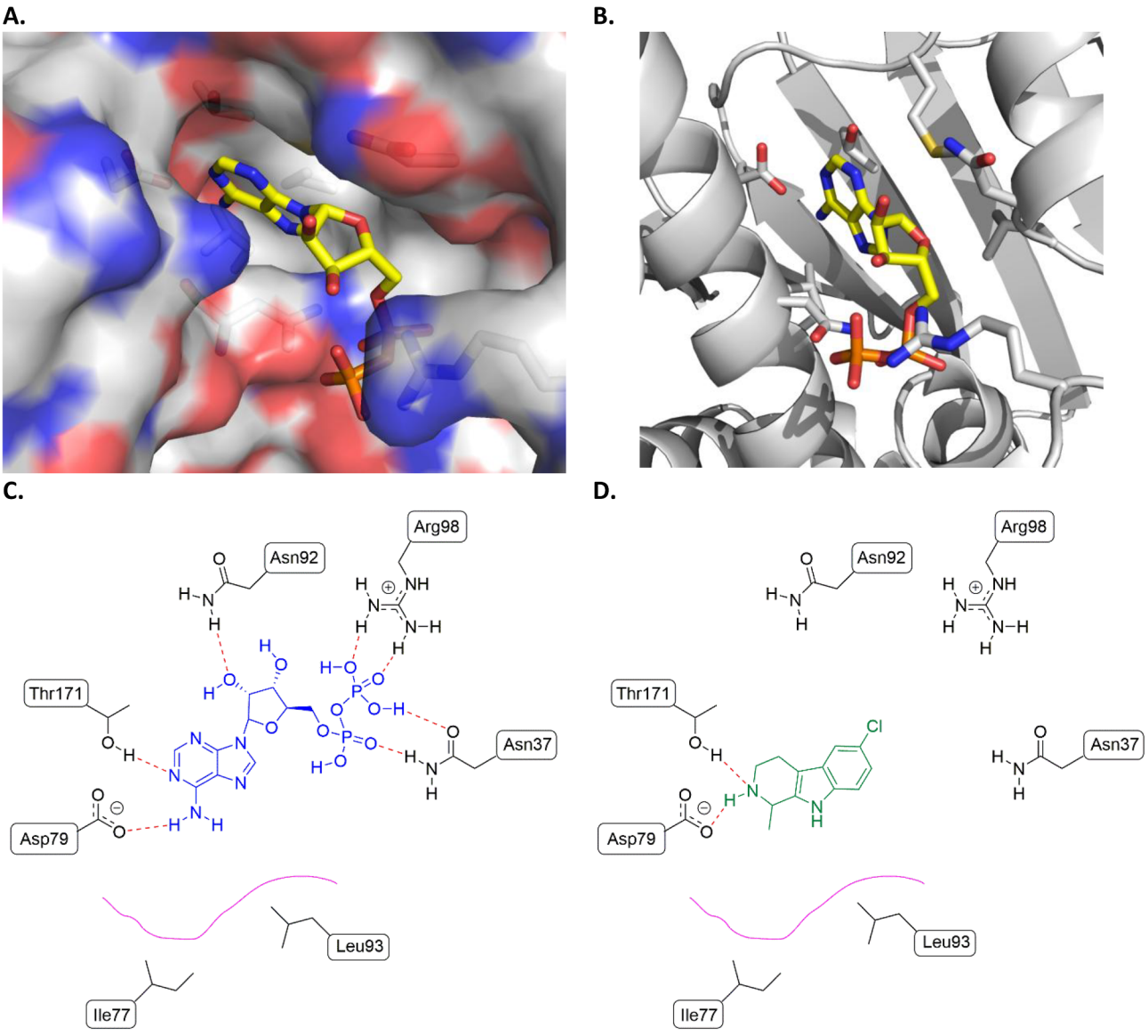

Fig. 2. Crystal structure of ADP bound to PfHsp90. (A) Three dimensional view of the top of the binding pocket surface of PfHsp90 with ADP. Red protein surfaces are oxygen atoms, blue are nitrogen atoms, and grey are carbon atoms. ADP is shown with a yellow backbone. (B) Binding pocket shown with the protein as a ribbon. (C) Two dimensional representation of ADP bound to PfHsp90. ADP is shown in blue, polar contacts are indicated by dotted red lines, and aliphatic regions indicated with pink. (D) Putative binding model of **1**.

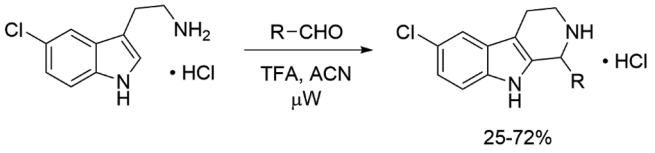

Scheme 1. Preparation of ring substituted derivatives of **1**.

We also investigated *N*-alkylation at the indole nitrogen with the goal of increasing the non-polar interactions.

To prepare analogs of **1** in which the methyl group was replaced by a variety of ring systems we utilized a previously reported synthesis of tetrahydro-β-carbolines via a microwave mediated Pictet-Spengler reaction[11] (Scheme 1).

To synthesize derivatives of **1** that were alkylated at the indole nitrogen, a protection-alkylation-deprotection strategy was used, as outlined in Scheme 2. While we were able to successfully isolate a methylated and ethylated derivative, attempts to alkylate using this methodology with larger alkyl groups lead to only trace product which could not be isolated in sufficient amounts to screen. While additional synthetic strategies could potentially yield more derivatives, we decided to screen the two compounds we had on hand first before expanding upon other *N*-alkylated products by alternative routes.

We then tested the proliferation inhibitory activity of our compounds against the chloroquine-sensitive *P. falciparum* 3D7 strain (MRA-102) in O-positive erythrocytes (Table 1). We also tested these compounds for inhibition of proliferation of a human fibroblast cell line (BJ).

The majority of phenyl-substituted derivatives displayed improved potency, typically around one order of magnitude better than **1**, with **7** presenting the best potency (352 nM) and an improvement of two orders of magnitude compared to **1**. Larger substituents including napthyl, benzyl, and cyclohexyl derivates showed little improvement, and indole *N*-alkylated compounds were completely inactive. Most compounds displayed little to no effect on the proliferation of the human BJ cell line.

To predict the binding mode of our new analogs, we docked our lead compound to the ATP pocket of PfHsp90 with the Vina[14] and iDock[15] programs. Default parameters were used for both docking programs as longer search times have demonstrated little improvement against known benchmarks.[16] Since our compounds are chiral, we docked both the (*R*) and (*S*) forms of **7**, with both programs predicting nearly identical poses for each enantiomer (Fig. 3). We were pleased to see that the computed binding pose of (*R*)-**7** fit as predicted, with the *meta*-tolyl ring residing in the aliphatic pocket and likely polar contacts between the piperidine nitrogen and the nearby Asp79 and Thr171 residues. The harmine core of (*R*)-**7** also resides in roughly the same position as the adenine ring of ADP. The (*S*)-**7** pose, however, was markedly different, with the harmine core rotated away from the pocket such that the indole nitrogen appears to interact with Asp79 while the piperidine nitrogen continues to maintain contact Thr171. Moreover, the chlorine atom appears to be orientated toward Arg98, suggesting a possible ion–dipole interaction. In addition to the different predicted poses, both programs also predicted stronger binding for the (*R*) form, with Vina favoring (*R*)-**7** by 0.70 kcal/mol, and iDock favoring (*R*)-**7** by 0.72 kcal/mol. While these results may suggest that the (*R*) form is more potent, we do not believe that our simulations alone are sufficient to make this conclusion without additional *in vitro* work utilizing enantiopure compounds.

Our simulations provide a rational SAR model that explains the antimalarial activity of our compounds. Replacing the methyl group of **1** with a phenyl ring allows for additional hydrophobic interactions, giving most phenyl-substituted derivatives improved activity. The relatively small size of the hydrophobic floor formed by Ile77 and Leu93 explains why substituting a larger benzyl or napthyl group is unfavorable, as shown by the lower activity displayed by **12–14**. The *meta*-methyl group in lead compound **7** appears to fit tightly in the aliphatic floor of the binding pocket in close proximity to Ile77. This close proximity and aliphatic environment provide a reasonable explanation for why other phenyl substitutions alter the binding orientation due to steric and/or electronic repulsion, effectively weakening the putative hydrogen bonding interactions with Thr171 and Asp79 which is the likely driver of binding affinity. Alkylation of the indole nitrogen also causes significant loss of activity either through unfavorable steric interactions or the loss of the hydrogen bonding interaction predicted between the (*S*) form and Asp79. Our docking models also suggest that the chlorine atom, which points away from the binding pocket, could serve as a useful functional handle for the addition of substituents which could form more favorable interactions with Arg98.

In conclusion, we were able to rationally design and synthesize a library of tetrahydro-β-carboline derivatives of our original lead compound **1** by appending various aromatic substitutions in order to make

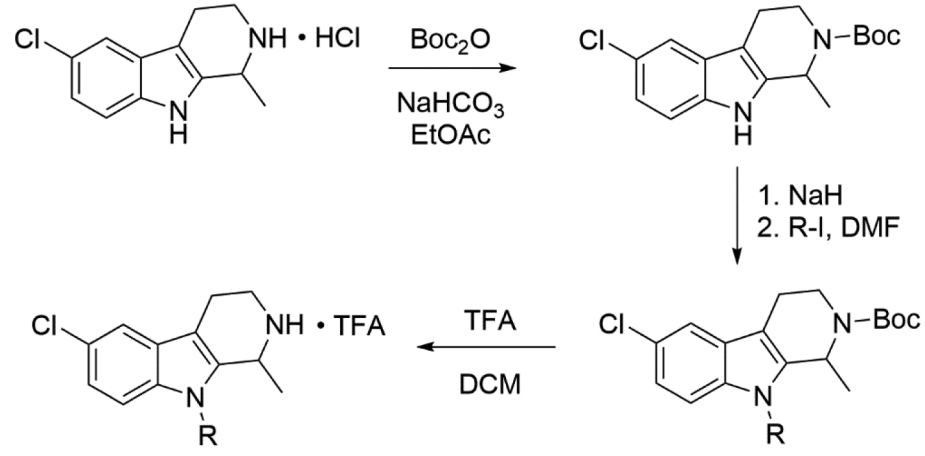

Scheme 2. Preparation of *N*-alkylated derivatives of **1**.

Table 1

Bioactivity, therapeutic index (T.I.) and cLogP values for all tested compounds.

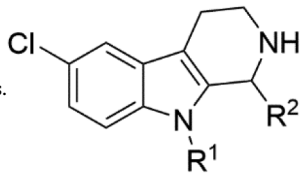

Compound	R^1	R^2	EC_{50} 3D7[a] (μM)	EC_{50} BJ[b] (μM)	T.I.	cLogP[c]
1	H	Me	12.2 ± 2.3[d]	–	–	2.05
2	H	Ph	1.67 ± 1.7	> 24	14	3.45
3	H	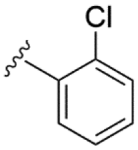	1.94 ± 1.09	> 24	12	4.00
4	H	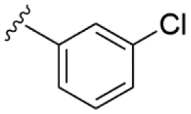	2.53 ± 0.75	23.6 ± 0.744	9	4.00
5	H	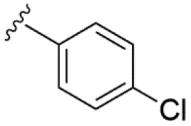	13.3 ± 0.495	23 ± 0.35	2	4.00
6	H	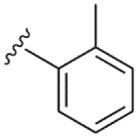	2.08 ± 2.03	> 24	12	3.93
7	H	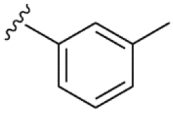	0.352 ± 0.487	> 24	68	3.93
8	H	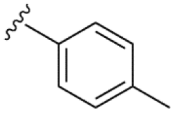	17.9 ± 0.088	> 24	1	3.93
9	H	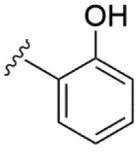	4.35 ± 1.22	15.7 ± 4.89	4	3.06
10	H	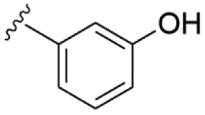	7.53 ± 1.0	> 24	3	3.06
11	H	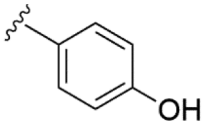	4.45 ± 0.423	> 24	5	3.06
12	H	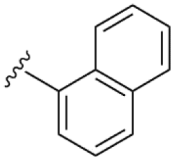	7.06 ± 2.34	> 24	3	4.44
13	H	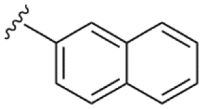	16.6 ± 2.03	17.2 ± 3.38	1	4.44
14	H	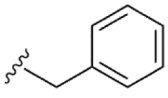	10.9 ± 1.15	> 24	2	3.72

(*continued on next page*)

Table 1 (*continued*)

Compound	R^1	R^2	EC_{50} 3D7[a] (μM)	EC_{50} BJ[b] (μM)	T.I.	cLogP[c]
15	H	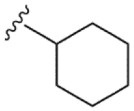	12.1 ± 5.25	> 24	2	3.69
16	Me	Me	> 18	> 24	1	2.29
17	Et	Me	> 18	> 24	1	2.62

[a] EC_{50} values are reported as the mean ± SD of five measurements. Assay endpoints were normalized from 0% (DMSO only) to 100% inhibition (16 μM Mefloquine).

[b] EC_{50} values are reported as the mean ± SD of six measurements. Assay endpoints were normalized from 0% (DMSO only) to 100% inhibition (58 μM Idarubicin).

[c] Calculated log P of the free base.

[d] Reported previously. See Ref. 12.

additional non-polar contacts. Our new front runner compound, **7**, displays a 35-fold increase in potency inhibiting proliferation of *P. falciparum* and no detectable antiproliferative activity against a human cell line. Docking simulations indicate that the most potent stereoisomer of **7** maintains the binding orientation of **1**, taking advantage of additional non-polar contacts in the ATP pocket of PfHsp90. While the gains in potency are notable, several challenges still remain with this scaffold. Future studies will include investigating other *meta*-substituted groups that are less sensitive to metabolism, additional functionalization utilizing the chloro group as a handle for coupling reactions, resolution of the two enantiomers such that they can be assayed independently, or oxidizing the compound to the achiral β-carboline system using a gentle oxidizing agent such as Ag_2CO_3 or IBX.[17]

Declaration of Competing Interest

The authors declare that they have no known competing financial interests or personal relationships that could have appeared to influence the work reported in this paper.

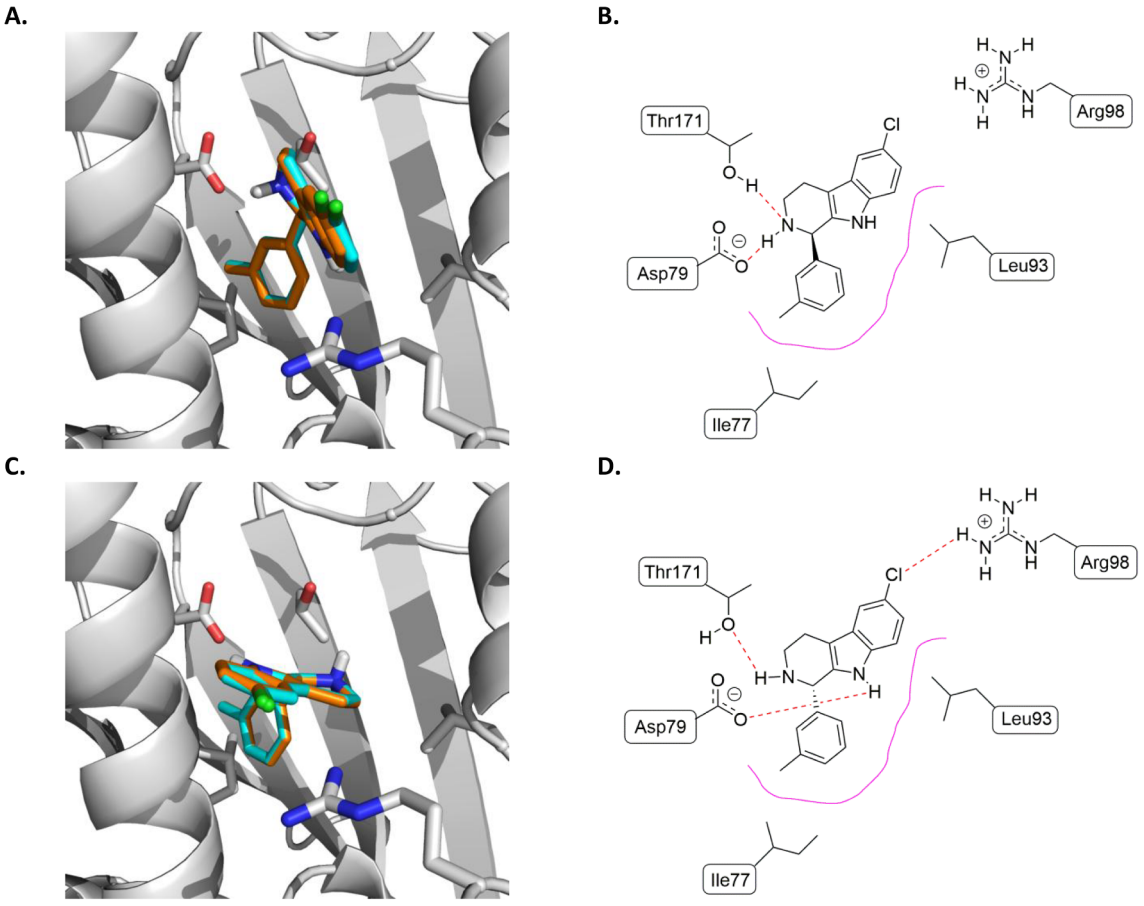

Fig. 3. Computed docking pose of lead compound **7** in the ATP pocket of PfHsp90. (A) Docking pose of (*R*)-**7** as calculated by Vina (gold backbone) and iDock (teal backbone). RMSD = 0.267 Å. (B) 2D representation for (*R*)-**7**, with polar interactions indicated by dotted red lines, and non-polar interactions shown as pink lines. (C) Docking pose of (*S*)-**7** as calculated by Vina (gold backbone) and iDock (teal backbone). RMSD = 0.096 Å. (D) 2D representation for (*S*)-**7**, with polar interactions indicated by dotted red lines, and non-polar interactions shown as pink lines.

Acknowledgements

This work was supported by the Center for Applied Biotechnology at California Polytechnic State University, the Bill and Linda Frost Fund and Grand Challenges Canada.

Appendix A. Supplementary data

Supplementary data to this article can be found online at https://doi.org/10.1016/j.bmcl.2020.127502.

References:

1. World Malaria Report 2019. World Health Organization; Geneva, Switzerland. 2019. https://www.who.int/publications-detail/world-malaria-report-2019.
2. Spangenberg T, Burrows JN, Kowalczyk S, McDonald S, Wells TN, Willis P. The open access malaria box: a drug discovery catalyst for neglected diseases. *PLoS One.* 2013;8:62901–62908.
3. Arama C, Troye-Blomberg M. The path of malaria vaccine development: challenges and perspectives. *J Intern Med.* 2014;275:456–466.
4. (a) Phillips MA, Burrows JN, Manyandoo C, van Huijsduijnen RH, van Voorhis WC, Wells TNC. *Malaria Nat Rev Dis Prim.* 2017;3:17050
(b) Durrows JN, Burlot E, Campo B, et al. Antimalarial Drug Discovery – the Path towards Eradication. *Parasitology.* 2014;141:128–139
(c) Flannery EL, Chatterjee AK, Winzeler EA. Antimalarial Drug Discovery: Approaches and Progress toward New Medicines. *Nat Rev Microbiol.* 2013;11:849–862
(d) Renslo AR. Antimalarial drug discovery: from quinine to the dream of eradication. *ACS Med Chem Lett.* 2013;4:1126–1128.
5. (a) Dondorp AM, Nosten F, Yi P, et al. Artemisinin resistance in plasmodium falciparum malaria. *N Engl J Med.* 2009;361:455–467
(b) Haldar K, Bhattacharjee S, Safekui I. Drug resistance in plasmodium. *Nat Rev Micro.* 2018;16:156–170.
6. Gamo FJ. Antimalarial drug resistance: new treatment options for *Plasmodium*. *Drug Dis Today: Technol.* 2014;11:81–88.
7. Shrestha L, Bolaender A, Patel HJ, Taldone T. Heat Shock Protein (HSP) Drug Discovery and Development: Targeting Heat Shock Proteins in Disease. *Curr Top Med Chem.* 2016;16:2753–2764.
8. Su XZ, Wellems TE. Sequence, Transcript Characterization and Polymorphisms of a *Plasmodium falciparum* Gene Belonging to the Heat-Shock Protein (Hsp) 90 Family. *Gene.* 1994;151:225–230.
9. Shahinas D, Liang M, Datti A, Pillai DR. A Repurposing Strategy Identifies Novel Synergistic inhibitors of *Plasmodium falciparum* Heat Shock Protein 90. *J Med Chem.* 2010;53:3552–3557.
10. Taldone T, Gozman A, Maharaj R, Chiosis G. Targeting Hsp90: Small-Molecule Inhibitors and their Clinical Development. *Curr Opin Phamacol.* 2008;8:370–374.
11. Shahinas D, Macmullin G, Benedict C, Crandall I, Pillai DR. Harmine is a Potent Antimalarial Targeting Hsp90 and Synergizes with Chloroquine and Artemisinin. *Antimicrob Agents Chemother.* 2012;56:4207–4213.
12. Eagon S, Anderson MO. Microwave-Assisted Synthesis of Tetrahydro-β-carbolines and β-Carbolines. *Eur J Org Chem.* 2014;8:1653–1665.
13. Bayih AG, Folefoc A, Mohon AN, Eagon S, Anderson M, Pillai DR. *In Vitro* and *in Vivo* Anti-malarial Activity of Novel Harmine-Analog Heat Shock Protein 90 Inhibitors: A Possible Partner for Artemisinin. *Malar J.* 2016;15:579.
14. Trott O, Olson AJ. AutoDock Vina: Improving the Speed and Accuracy of Docking with a New Scoring Function, Efficient Optimization, and Multithreading. *J Comput Chem.* 2010;31:455–461.
15. Li H, Leung K, Wong M. iDock: A Multithreaded Virtual Screening Tool for Flexible Ligand Docking. *CIBCB.* 2015;34:115–126.
16. Masters L, Eagon S, Heying M. Evaulation of Consensus Scoring Methods for AutoDock Vina, Smina and iDock. *J Mol Graph Model.* 2020;96:107532.
17. (a) Durham SD, Sierra B, Gomez MJ, et al. Synthesis of β-Carbolines via a Silver-Mediated Oxidation of Tetrahydro-β-carbolines. *Tetrahedron Lett.* 2017;58:2747–2750
(b) Panarese JD, Waters SP. Tandem Iodine-Mediated Oxidations of Tetrahydro-β-carbolines: Total Synthesis of Eudistomins Y1–Y7. *Org Biomol Chem.* 2013;11:3428–3431.